

Multihead Multitrack Detection with Reduced-State Sequence Estimation

Bing Fan, Hemant K. Thapar, and Paul H. Siegel

Center for Magnetic Recording Research, University of California, San Diego, La Jolla, CA 92093, USA
 bifan@ucsd.edu, hemantkthapar@gmail.com, psiegel@ucsd.edu

Abstract—In shingled magnetic recording (SMR), the multi-head multitrack (MHMT) detector can better combat the effect of intertrack interference (ITI) than the single-head single-track (SHST) detector. Such a detector, however, has prohibitive implementation complexity. In this paper we propose to use the reduced-state sequence estimation (RSSE) algorithm to significantly reduce the complexity, and render MHMT practical. A commonly used symmetric two-head two-track (2H2T) channel model is considered in this work. Well-structured reduced-state trellises are constructed by evaluating the effective symbol pair distances and designing proper set partitioning principles. Different trellis configurations are obtained based on the desired performance/complexity tradeoff. Simulation results show that the MHMT detector can achieve near maximum-likelihood (ML) performance with a small fraction of the original number of trellis states.

Index Terms—Shingled Magnetic Recording, Intersymbol Interference, Intertrack Interference, Viterbi Algorithm.

I. INTRODUCTION

Intertrack interference (ITI) is one of the more severe impairments in shingled magnetic recording (SMR). This impairment is best handled using a multihead array and jointly processing multiple tracks [1]. The associated detector complexity is, however, drastically increased.

Consider a symmetric two-head two-track (2H2T) system described by

$$\begin{bmatrix} r^a(D) \\ r^b(D) \end{bmatrix} = \begin{bmatrix} 1 & \epsilon \\ \epsilon & 1 \end{bmatrix} \begin{bmatrix} x^a(D)h(D) \\ x^b(D)h(D) \end{bmatrix} + \begin{bmatrix} n^a(D) \\ n^b(D) \end{bmatrix}, \quad (1)$$

where $x^a(D)$, $x^b(D)$ are the data sequences independently recorded on two adjacent tracks a and b , with $x^i(D) = \sum_{k=0}^N x_k^i D^k$ and $x_k^i \in \{-1, +1\}$ for $i \in \{a, b\}$. Each single track is equalized to the same target $h(D) = h_0 + h_1 D + \dots + h_\nu D^\nu$, and the ITI effect is characterized by a parameter ϵ . The received sequences from two heads, $r^a(D)$ and $r^b(D)$, are added with the electronic noise, $n^a(D)$ and $n^b(D)$. We assume $n^a(D)$ and $n^b(D)$ are uncorrelated and i.i.d, with $n_k^a, n_k^b \sim \mathcal{N}(0, \sigma^2)$.

The maximum-likelihood (ML) 2H2T detector simultaneously decodes two tracks by searching a joint trellis [1] [2] [3]. Let $\mathbf{x}_k = (x_k^a, x_k^b)$ denote one input symbol of the 2H2T system. The possible input symbols form a two dimensional 4-symbol constellation. This extended input set causes exponential increase in the computation complexity. For a channel with

memory ν , the ML trellis has 4^ν states, each with 4 incoming and outgoing edges. Compared to the traditional single-head single-track (SHST) detector with complexity $O(2^\nu)$, the ML 2H2T detector operates at $O(4^\nu)$. For $\nu > 3$, which is typical in practical recording channels, the ML 2H2T detector becomes impractical. In the following discussion we use the number of trellis states as a measure of the operational complexity of a detector.

In this work we consider the design of detectors that use fewer trellis states while retaining good performance. Reduced-State Sequence Estimation (RSSE) was proposed in [4] to reduce the detection complexity when the system has a large input signal set and/or a long channel response. The algorithm was designed primarily for transmitting complex symbols, drawn from the quadrature amplitude modulation (QAM) constellation, through a partial response channel. In this work we will show that the RSSE algorithm can be modified and applied to the 2H2T system to significantly reduce the detection complexity. Our simulation results show that, with fewer than half the number of the states of the full MLSE, RSSE can achieve near-ML performance on many channels. Moreover, the evaluation of RSSE performance is tractable through use of error events analysis. (Due to space limitations, this analysis will be presented in a subsequent paper.)

The paper is organized as follows. In Section II we first briefly review the traditional RSSE algorithm for the QAM system. Next we show how to construct reduced-state trellises for the 2H2T channel by redefining the distance measure in the input constellation and designing proper set partitioning rules. In Section III we construct different trellis configurations based on the performance/complexity tradeoff, and simulate the RSSE detector on several channels with different channel polynomials.

II. 2H2T DETECTOR WITH RSSE

A. Review of RSSE

The traditional RSSE is designed for transmitting QAM symbols through an ISI channel with channel memory ν . Recall that in the ML detector, the trellis state is represented as a length ν vector,

$$\mathbf{p}_n = [\mathbf{x}_{n-1}, \mathbf{x}_{n-2}, \dots, \mathbf{x}_{n-\nu}], \quad (2)$$

where each symbol \mathbf{x}_{n-k} is complex-valued, and selected from a two-dimensional signal set \mathcal{C} whose size is M . In

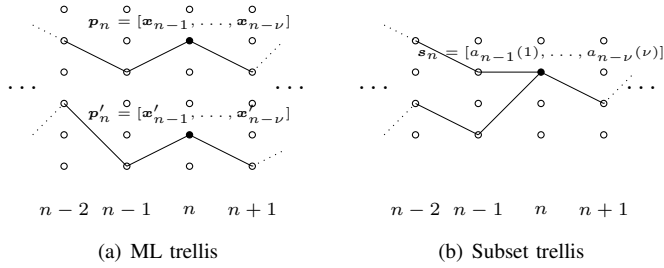


Fig. 1. Comparison between the decoding paths on (a) ML trellis and (b) subset trellis. If at time n two paths ending at ML states \mathbf{p}_n and \mathbf{p}'_n satisfy $\mathbf{x}_{n-k} \in a_{n-k}(k)$ and $\mathbf{x}'_{n-k} \in a_{n-k}(k)$ for all $k = 1, \dots, \nu$, then they will merge early at subset state \mathbf{s}_n in the subset trellis.

RSSE, to reduce the number of trellis states, several ML states are grouped into a **subset state**. To do this, for the k th element \mathbf{x}_{n-k} in \mathbf{p}_n , a set partition $\Omega(k)$ of \mathcal{C} is defined, and \mathbf{x}_{n-k} is represented by its subset index $a_{n-k}(k)$ in $\Omega(k)$. Notice that $\Omega(k)$ can be different for $k = 1, \dots, \nu$. Let $J_k = |\Omega(k)|$ be the number of subsets in partition $\Omega(k)$, $1 \leq J_k \leq M$. Then the subset index $a_{n-k}(k)$ can take its value from $0, 1, \dots, J_k - 1$. The corresponding subset state of \mathbf{p}_n is denoted by

$$\mathbf{s}_n = [a_{n-1}(1), a_{n-2}(2), \dots, a_{n-\nu}(\nu)]. \quad (3)$$

The trellis constructed from all possible \mathbf{s}_n is called the **subset trellis**. To obtain a well-defined trellis structure, the partition $\Omega(k)$ is restricted to be a further partition of the subsets in $\Omega(k+1)$, for $1 \leq k \leq \nu - 1$. This condition guarantees that for a given state \mathbf{s}_n and current input \mathbf{x}_n , the next subset state is uniquely determined and represented as

$$\mathbf{s}_{n+1} = [a_n(1), a_{n-1}(2), \dots, a_{n-\nu+1}(\nu)], \quad (4)$$

where $a_n(1)$ is the subset index of \mathbf{x}_n in $\Omega(1)$, $a_{n-1}(2)$ is the index of \mathbf{x}_{n-1} in $\Omega(2)$, and so on. The number of states in the subset trellis is $\prod_{k=1}^{\nu} J_k$. The complexity of a RSSE trellis can be controlled by specifying ν parameters, J_k for $1 \leq k \leq \nu$. We define the **configuration** of a subset trellis to be a vector $\mathbf{J} = [J_1, J_2, \dots, J_\nu]$. A valid configuration satisfies $J_1 \geq J_2 \geq \dots \geq J_\nu$.

To apply the Viterbi algorithm (VA) on a subset trellis, a decision feedback scheme is introduced to calculate the branch metric, since the subset state \mathbf{s}_n does not uniquely specify the most recent ν symbols. During the detection process, a modified path history is used to store the surviving symbol $\hat{\mathbf{x}}_{n-1}$ that leads to state \mathbf{s}_n . The actual surviving ML state $\hat{\mathbf{p}}_n$ is obtained by tracing back ν steps in the path history. Error propagation may occur in this process, but its effect is negligible [4] [5].

The underlying idea of RSSE is to drop less likely paths early in the detection process. Since each subset state contains multiple ML states, certain paths will merge earlier in the subset trellis than in the ML trellis, as shown in Fig. 1. If $J_k = M$ for $1 \leq k \leq \nu$, RSSE becomes MLSE. Otherwise it is suboptimal. To minimize the performance loss, proper set partitions $\Omega(k)$ should be selected carefully to guarantee that enough distance differences have been accumulated to reliably distinguish between merging paths. For the M -QAM system, it is

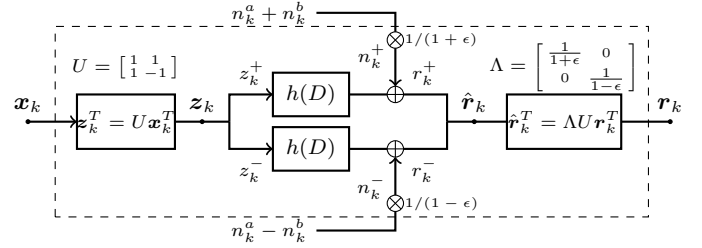


Fig. 2. A schematic of the WSSJD model. Coordinate transformations are applied in the input space ($\mathbf{z}_k^T = U\mathbf{x}_k^T$) and the output space ($\hat{\mathbf{r}}_k^T = \Lambda U\mathbf{r}_k^T$). They decompose the original 2H2T system into the sum channel (upper branch) and the subtract channel (lower branch).

suggested that good performance can generally be obtained by maximizing the minimum intrasubset Euclidean distance for each partition $\Omega(k)$, $k = 1, \dots, \nu$ [4]. The Ungerboeck set partition tree [6] is shown to have this property and is adopted to make the selection of $\Omega(k)$. For more details about the subset trellis construction for the M -QAM system, the reader is referred to [4].

The use of the Ungerboeck set partition tree is key to obtaining good performance of the RSSE algorithm on the QAM system. However, such a set partition tree cannot be directly applied to the 2H2T system because of the ITI. In the next subsection we will show that a simple transformation can decompose the original 2H2T system into two independent channels, resulting in a QAM-like structure. Then, instead of using the Euclidean distance, we define a new distance measure between the input symbols, based on which we construct a more suitable set partition tree for the 2H2T system.

B. Set Partition Tree for 2H2T System

In [7] we show that the 2H2T channel described by equation (1) is equivalent to

$$\begin{aligned} r^+(D) &= z^+(D)h(D) + n^+(D) \\ r^-(D) &= z^-(D)h(D) + n^-(D), \end{aligned} \quad (5)$$

where

$$\begin{bmatrix} z_k^+ \\ z_k^- \end{bmatrix} = \begin{bmatrix} 1 & 1 \\ 1 & -1 \end{bmatrix} \begin{bmatrix} x_k^a \\ x_k^b \end{bmatrix} \quad (6)$$

$$\begin{bmatrix} r_k^+ \\ r_k^- \end{bmatrix} = \begin{bmatrix} \frac{1}{1+\epsilon} & 0 \\ 0 & \frac{1}{1-\epsilon} \end{bmatrix} \begin{bmatrix} 1 & 1 \\ 1 & -1 \end{bmatrix} \begin{bmatrix} r_k^a \\ r_k^b \end{bmatrix} \quad (7)$$

$$\begin{bmatrix} n_k^+ \\ n_k^- \end{bmatrix} = \begin{bmatrix} \frac{1}{1+\epsilon} & 0 \\ 0 & \frac{1}{1-\epsilon} \end{bmatrix} \begin{bmatrix} 1 & 1 \\ 1 & -1 \end{bmatrix} \begin{bmatrix} n_k^a \\ n_k^b \end{bmatrix}. \quad (8)$$

Let $\mathbf{x}_k = (x_k^a, x_k^b)$ and $\mathbf{r}_k = (r_k^a, r_k^b)$ be the input and received symbols of the original system (1) and let $\mathbf{z}_k = (z_k^+, z_k^-)$ and $\hat{\mathbf{r}}_k = (r_k^+, r_k^-)$ denote the input and received symbols of the transformed system (5). Their equivalence is visually indicated in Fig. 2. The noise components of the transformed system, n_k^+ and n_k^- , are independent, but with different noise power, $n_k^+ \sim \mathcal{N}(0, \frac{\sigma^2}{(1+\epsilon)^2})$, $n_k^- \sim \mathcal{N}(0, \frac{\sigma^2}{(1-\epsilon)^2})$.

The ML trellis of the transformed system is formed by all possible $\mathbf{p}_n = [z_{n-1}, \dots, z_{n-\nu}]$. ML detection on this new

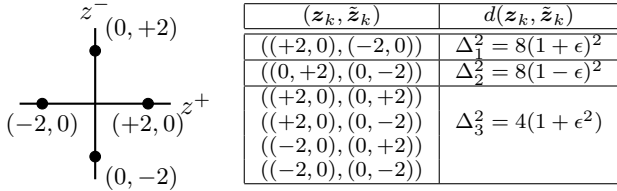


Fig. 3. The input constellation (left) and the ESPDs (right).

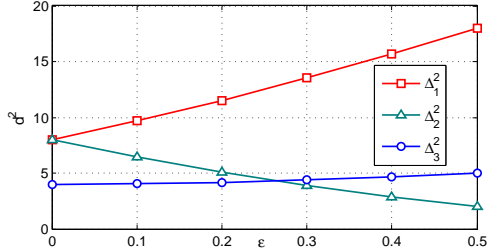


Fig. 4. ESPDs as functions of ϵ

channel model is called **weighted sum subtract joint detection** (WSSJD), summarized as follows:

- 1) Calculate $r^+(D)$ and $r^-(D)$ using equation (7).
- 2) To apply VA on the WSSJD trellis, weight the branch metrics

$$m(\mathbf{p}_n, \mathbf{p}_{n+1}) = (1 + \epsilon)^2 (r_n^+ - y_n^+)^2 + (1 - \epsilon)^2 (r_n^- - y_n^-)^2, \quad (9)$$

where $y_n^+ = \sum_{i=0}^{\nu} h_i z_{n-i}^+$ and $y_n^- = \sum_{i=0}^{\nu} h_i z_{n-i}^-$ are the noiseless ISI channel outputs. Choose the path with the smallest metric and decode to the estimates $\hat{z}^+(D)$ and $\hat{z}^-(D)$.

- 3) Calculate $\hat{x}^a(D)$ and $\hat{x}^b(D)$ using equation (6).

WSSJD is shown to have the same performance as the ML detector. Therefore, in the simulation we use WSSJD as a MLSE substitute for the 2H2T system, and the subset trellis is also constructed by considering the WSSJD inputs/outputs. As we will see, the coordinate transformations in WSSJD make it easier to measure the distances between symbols, which plays an important role in designing the set partition tree. However, the applicability of RSSE to the standard 2H2T ML detector holds. With a little abuse of notation, when we mention the ‘‘ML trellis,’’ we refer to the full ‘‘WSSJD trellis.’’ For more information, the reader is referred to [7].

The transformations in WSSJD decompose the original 2H2T system into two parallel channels. The sum channel and the subtract channel correspond to transmitting $z^+(D)$ and $z^-(D)$ through $h(D)$, respectively. Recall that in the QAM system, the real and imaginary components of a complex symbol are also transmitted through the channel independently. Therefore, z_k^+ and z_k^- can be treated as the real and imaginary components of a complex symbol z_k . The only difference from the QAM system is that the sum and the subtract channels have different signal-to-noise ratios (SNRs). The sum channel is less noisy, which results in more reliable early merge than the subtract channel. Considering this di-

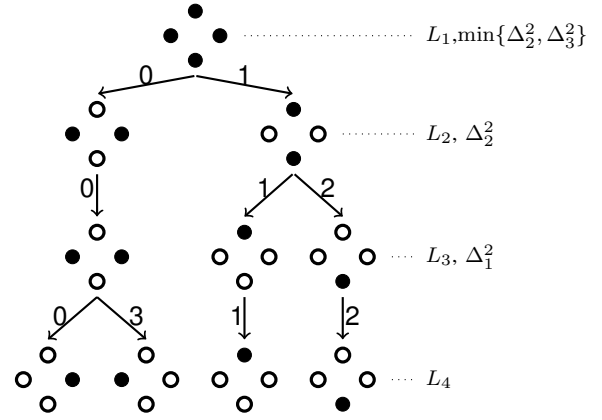


Fig. 5. The modified set partition tree. This tree contains 4 levels, $\{L_1, L_2, L_3, L_4\}$, each of which is a set partition of the WSSJD input constellation. The minimum ESPD on each level is specified on the right side. The number associated with each branch is the index of the subset in the corresponding set partition.

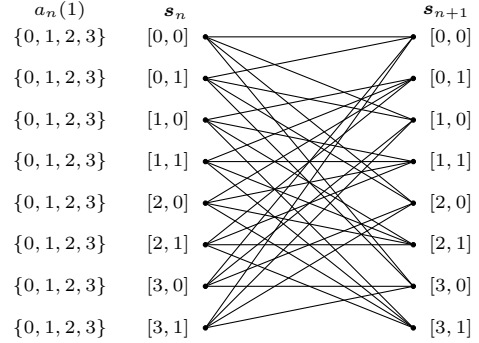


Fig. 6. Subset trellis with configuration [4,2] on memory-2 channel.

mensional asymmetry, instead of using a Euclidean distance we define the **effective symbol pair distance** (ESPD)

$$d^2(z_k, \tilde{z}_k) = \frac{(1 + \epsilon)^2}{2} (z_k^+ - \tilde{z}_k^+)^2 + \frac{(1 - \epsilon)^2}{2} (z_k^- - \tilde{z}_k^-)^2. \quad (10)$$

The input constellation and the ESPDs between different pairs of symbols are shown in Fig. 3. Notice that ESPDs can change with respect to ϵ , as shown in Fig. 4. Therefore even with the same subset trellis configuration, the RSSE performs differently at different ITI levels.

The set partition tree designed for 2H2T is constructed by maximizing the minimum intrasubset ESPD on each level, which results in an unbalanced tree shown in Fig. 5. Compared to the Ungerboeck set partition tree, the additional level L_3 comes from the asymmetric distance measure in the z^+ and z^- dimensions, and it provides more flexibility in choosing set partitions, which leads to a better performance/complexity tradeoff.

To construct the subset trellis, $\Omega(k)$ should be chosen from the set partition tree for $k = 1, \dots, \nu$. As an example, Fig. 6 shows an eight-state subset trellis for a memory-2 channel with configuration [4, 2], i.e., $\Omega(1)$ is chosen to be L_4 , and $\Omega(2)$ is chosen to be L_2 . In this case, the incoming symbols start to merge at the second stage. For a configuration with $J_1 < 4$,

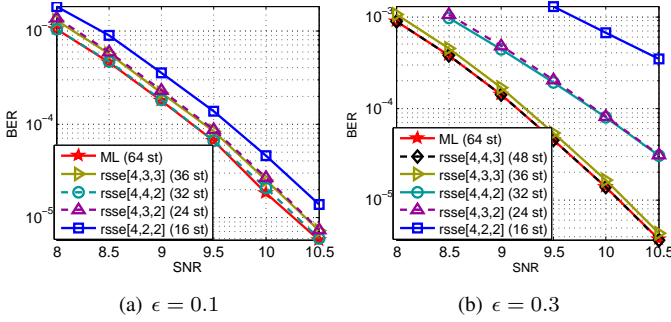


Fig. 7. Performance comparison between RSSE and ML detector on EPR4 channel at different ITI levels. The legend shows the RSSE subset trellis configuration and the corresponding number of trellis states.

two different input symbols z_n and \tilde{z}_n can belong to the same subset $a_n(1)$. The resulting subset trellis will contain parallel branches. The early merge happens at every step, when RSSE needs to select the survivor symbol between parallel branches. The performance of RSSE algorithm on different subset trellises is shown in the next section.

III. SIMULATION RESULTS

We examine the RSSE performance on two types of channels at different ITI levels. The SNR is defined as

$$\text{SNR}(\text{dB}) = 10 \log \frac{\|h(D)\|^2}{2\sigma^2} \quad (11)$$

A. EPR4 channel

For the EPR4 channel $h(D) = 1 + D - D^2 - D^3$, we apply RSSE to several subset trellises with different complexities. The resulting bit error rate (BER) vs. SNR performance at different ITI levels is plotted in Fig. 7. The comparison between Figs. 7(a) and Figs. 7(b) shows that even using the same subset trellis, RSSE performs differently under different ITI levels, and its performance correlates with the minimum intrasubset ESPDs of the set partitions configured in the subset trellis. At a low ITI level ($\epsilon = 0.1$), the performance of RSSE on subset trellis [4, 4, 2] coincides with that of the ML detector. The BER curves of [4, 3, 3] and [4, 3, 2] overlap, and are both within 0.1dB away from the ML curve. Subset trellis [4, 2, 2] further reduces the number of states to 16, but incurs a 0.3dB loss. When the ITI level becomes higher ($\epsilon = 0.3$), the subset trellis [4, 4, 2] cannot provide reliable early path merging because the minimum intrasubset ESPD Δ_2^2 in $\Omega(3) = L_2$ is substantially reduced. However, a less aggressive construction using configuration [4, 4, 3] achieves near-ML performance. The decrease in Δ_2^2 at this ITI level also degrades the performance of RSSE[4, 2, 2] and [4, 3, 2]. Their BER curves overlap in Figs. 7(b). In contrast, the increase of Δ_1^2 brings [4, 3, 3] closer to the ML performance, compared to the case $\epsilon = 0.1$.

Similarly, for the PR2 channel $h(D) = 1 + 2D + D^2$, simulation results show that the BER curve of RSSE[4, 2] essentially overlaps with that of the ML detector at $\epsilon = 0.1$. For $\epsilon = 0.3$, RSSE[4, 3] essentially achieves ML performance.

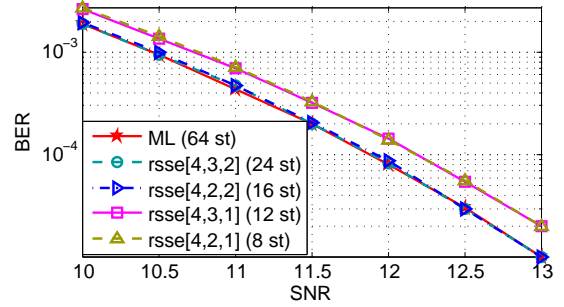


Fig. 8. Performance comparison between RSSE and ML detector on minimum phase channel $h(D) = 1 + 1.6D + 1.1D^2 + 0.4D^3$, at $\epsilon = 0.1$.

B. Minimum phase channels

Minimum phase channels can better model the real channel on a disk drive. Using the whitened matched filter [8], we derive a memory-3 minimum phase channel polynomial $h(D) = 1 + 1.6D + 1.1D^2 + 0.4D^3$. Since the minimum phase condition implies that most of the channel energy is distributed over the most recent samples, the early merge in RSSE can be more reliable compared to the linear phase channel. As shown in Fig. 8, ML, RSSE[4, 3, 2], and RSSE[4, 2, 2] have essentially identical performance. In particular, RSSE[4, 2, 2] performs much better on the minimum phase channel than on the EPR4 channel, allowing RSSE to achieve near-ML performance with only 16 states. Other more aggressive configurations are also shown in Fig. 8. As can be seen, RSSE with only 8 states can achieve performance that is within 0.3dB of ML detection.

ACKNOWLEDGMENT

This work was supported in part by the National Science Foundation under Grant CCF-1405119, and the Center for Magnetic Recording Research at UC San Diego.

REFERENCES

- [1] E. Soljanin and C. Georghiades, "Multihead detection for multitrack recording channels," *IEEE Trans. Inf. Theory*, vol. 44, no. 7, pp. 2988–2997, Nov. 1998.
- [2] X. Ma and L. Ping, "Iterative detection/decoding for two-track partial response channels," *IEEE Commun. Lett.*, vol. 8, no. 7, pp. 464–466, Jul. 2004.
- [3] L. Barbosa, "Simultaneous detection of readback signals from interfering magnetic recording tracks using array heads," *IEEE Trans. Magn.*, vol. 26, no. 5, pp. 2163–2165, Sep. 1990.
- [4] M. Eyuboglu and S. Qureshi, "Reduced-state sequence estimation with set partitioning and decision feedback," *IEEE Trans. Commun.*, vol. 36, pp. 13–20, Jan. 1988.
- [5] W.-H. Sheen and G. L. Stuber, "Error probability for reduced-state sequence estimation," *IEEE J. Sel. Areas Commun.*, vol. 10, no. 3, pp. 571–578, Apr. 1992.
- [6] G. Ungerboeck, "Channel coding with multilevel/phase signals," *IEEE Trans. Inf. Theory*, vol. 28, no. 1, pp. 55–67, Jan. 1982.
- [7] B. Fan, H. K. Thapar, and P. H. Siegel, "Multihead multitrack detection in shingled magnetic recording with ITI estimation," in *Proc. IEEE Int. Conf. Commun. (ICC)*, London, UK, Jun. 2015, to appear.
- [8] G. D. Forney, "Maximum-likelihood sequence estimation of digital sequences in the presence of intersymbol interference," *IEEE Trans. Inf. Theory*, vol. 18, no. 3, pp. 363–378, May 1972.